EARTH SURFACE PROCESSES AND LANDFORMS
Earth Surf. Process. Landforms (2010)

Published online in Wiley InterScience
(www.interscience.wiley.com) DOI: 10.1002/esp.1937

Shear-rate-dependent strength control on the dynamics of rainfall-triggered landslides, Tokushima Prefecture, Japan

Gonghui Wang,[1]* Akira Suemine[1] and William H. Schulz[2†]
[1] Disaster Prevention Research Institute, Kyoto University
[2] United States Geological Survey, Denver, CO, USA

Received 15 February 2009; Revised 1 September 2009; Accepted 14 September 2009

*Correspondence to: Gonghui Wang, Research Centre on Landslides, Disaster Prevention Research Institute, Kyoto University, Gokasho, Uji, Kyoto, 611, Japan.
E-mail: wanggh@landslide.dpri.kyoto-u.ac.jp
†The contribution of William H. Schulz to this article was prepared as part of his duties as a United States Federal Government employee.

ESPL
Earth Surface Processes and Landforms

ABSTRACT: A typhoon (Typhoon No. 10) attacked Shikoku Island and the Tyugoku area of Japan in 2004. This typhoon produced a new daily precipitation record of 1317 mm on Shikoku Island and triggered hundreds of landslides in Tokushima Prefecture. One catastrophic landslide was triggered in the Shiraishi area of Kisawa village, and destroyed more than 10 houses while also leaving an unstable block high on the slope. The unstable block kept moving after the event, showing accelerating and decelerating movement during and after rainfall and reaching a displacement of several meters before countermeasures were put into place. To examine the mechanism for this landsliding characteristic, samples (weathered serpentinite) were taken from the field, and their shear behaviours examined using ring shear tests. The test results revealed that the residual shear strength of the samples is positively dependent on the shear rate, which may provide an explanation for the continuous accelerating–decelerating process of the landsliding. The roughness of the shear surface and the microstructure of the shear zone were measured and observed by laser microscope and SEM techniques in an attempt to clarify the mechanism of shear rate effect on the residual shear strength. Copyright © 2010 John Wiley & Sons, Ltd.

KEYWORDS: creep movement; serpentinite landslide; residual shear strength; rate effect; mechanism

Introduction

Typhoon Namtheun (the 10th tropical storm in the western Pacific in 2004) originated west of Minamitorishima Island of Japan on 25 July 2004. It made landfall on Shikoku Island on 31 July (Figure 1a), then passed through the Seto Inland Sea and Hiroshima Prefecture, and moved toward the eastern part of the Korean Peninsula, losing energy to become a tropical depression. Accompanying this typhoon, heavy rain fell on the Shikoku area of Japan (Figure 1b), especially in the surrounding area of Kisawa village (on the south-west part) of Tokushima Prefecture. The total precipitation from July 30 to August 2 was more than 2000 mm (Figure 2). This is several times the normal precipitation for the months of July and August in this area. Hourly precipitation reached more than 120 mm (Figure 2). The highest daily precipitation of 1317 mm was recorded on 1 August; this value exceeds the previous Japanese daily precipitation record of 1114 mm, recorded at Kito village (about 16 km southwest of Kisawa village) on 11 September 1976 accompanying Typhoon Fran.

The area where total storm precipitation exceeded 1500 mm was centered on Kisawa village and Kaminaka town, within a narrow area of 5–6 km in the east–west direction, and 10–20 km in the south–north direction (Figure 1b). In this area, many landslides were triggered (Wang *et al.*, 2005), including a catastrophic failure that occurred in the upper part of Furon Valley, Shiraishi district and destroyed more than 10 houses. A slow, intermittently moving landslide remained immediately uphill from the catastrophic landslide source area. This upper landslide occupied the gently sloping (about 12°), upper part of the valley and its basal sliding surface occurred within weathered serpentinite. The landslide was actively moving after the typhoon, exposing the downstream residents to danger. Acknowledging the risk, the residents were ordered to evacuate and countermeasures were started immediately after the August event. Displacement monitoring revealed that the upper landslide experienced accelerating and decelerating movement during and after each rainfall. Although the accumulated displacement reached several meters and small, rapid landsliding occurred repeatedly in the lower part of the landslide, its main body did not suffer rapid, catastrophic failure. These movement characteristics are very rare for landslides in areas of Japan underlain by serpentinite. To clarify the movement mechanism, we took samples from the landslide area and examined their residual shear strength characteristics by means of ring shear tests. These tests were performed at various shear rates to examine possible effects on shear strength. We evaluated the structure of the shear

zones produced during ring shear tests using laser and scanning electron microscopes.

Landslides in the Shiraishi Area

The Shiraishi area was designated by the Japanese government as a landslide prevention area during 1962 in accordance with the Japanese Landslide Preventive Means, and the mountain stream flowing through the area was designated as a debris-flow-risk-rich stream (Figure 3). The rapid, catastrophic landslide triggered by Typhoon Namtheun rainfall in the upper part of the Furon Valley occurred around 20:00 on 1 August (hereinafter termed the first landslide). This landslide was 70 m in length, 35 m in width, and 2–3 m in depth, and originated where the valley floor sloped approximately 29° (Hiura *et al.*, 2004). The headscarp of the first landslide was at an elevation of 540 m and the toe of its deposit was at an elevation of 290 m, having reached the national road, and its horizontal travel distance was about 550 m. The landslide mass that reached the residential area totaled approximately 3300–4700 m^3. The landslide movement transformed from slide to flow when the slide reached the lower part of the slope. Many houses were destroyed or damaged by this event (Figure 4). Fortunately, the residents of this area noticed some unusual phenomena (such as groundwater flowing out from the middle part of the mountain slope and the sound of moving rocks), and then, recognizing the landslide risk, they started to evacuate at 15:00 on the day of the failure. Therefore, there was neither fatality nor injury (Hiura *et al.*, 2004). However, after this landslide-debris flow event occurred on 1 August, an unstable block (hereinafter termed Shiraishi landslide, which is the subject of this study) formed immediately upslope in the upper part of Furon Valley (Figure 4) and showed very active movement. Due to the great risk posed by

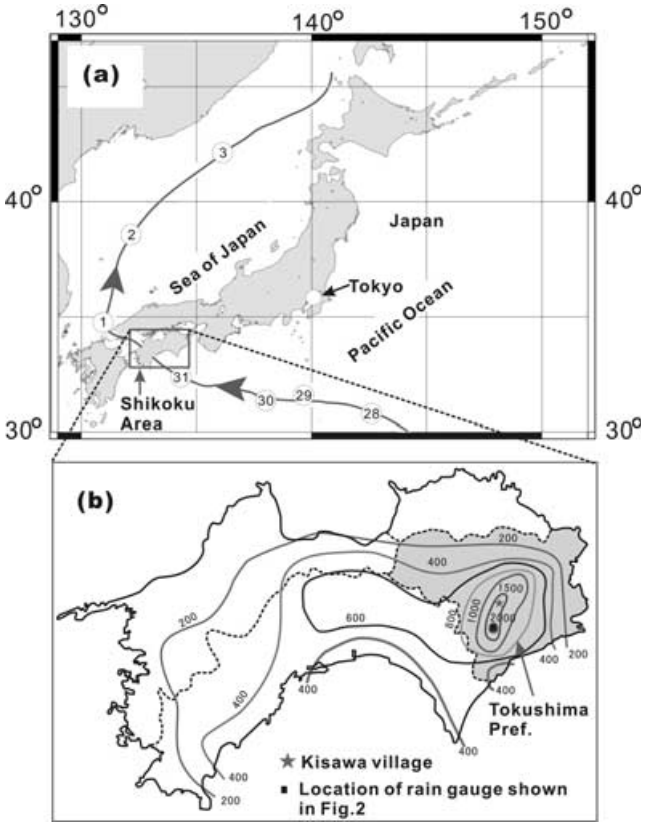

Figure 1. Rainfall distribution in the Shikoku area from 30 July to 2 August 2004, during the typhoon Namtheum (after Nakagawa River Office, Shikoku Development Bureau, Ministry of Land, Infrastructure, Transport and Tourism, Japan).

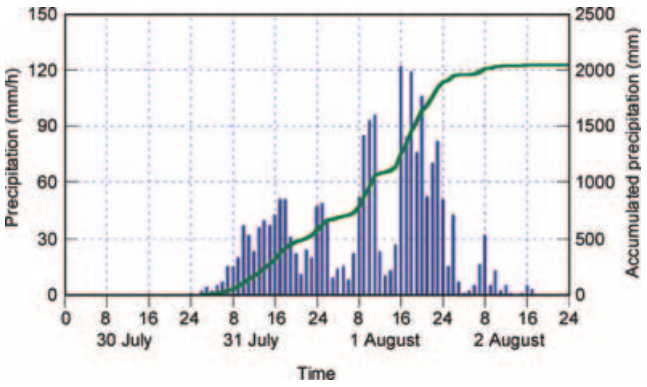

Figure 2. Hyetograph of the heavy rainfall (data courtesy of Shikoku Electric Power Co., Inc.). This figure is available in colour online at www.interscience.wiley.com/journal/espl

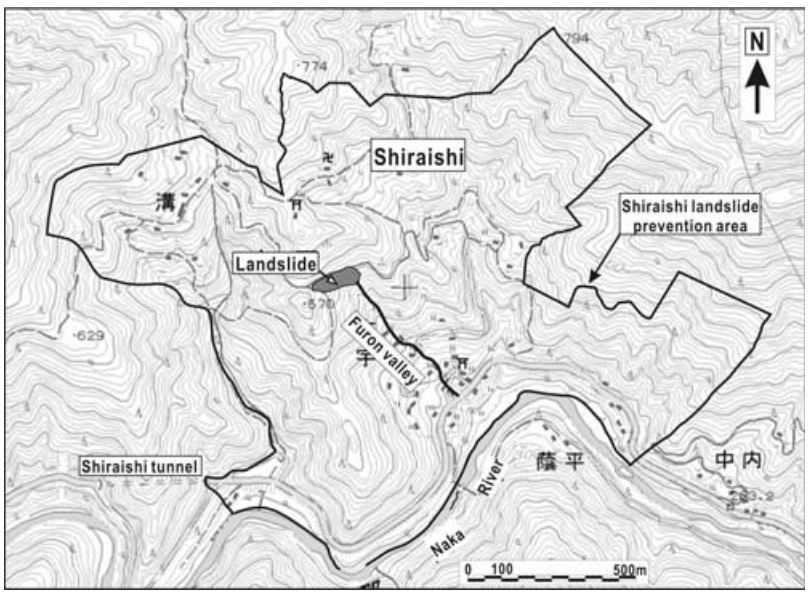

Figure 3. Shiraishi landslide prevention area and the location of the landslide in the Furon Valley.

this landslide (potential hazard area is shown on Figure 4), the downstream residents were ordered to evacuate until the landslide risk had been eliminated 2 years later.

Figure 5 presents a map of the landslide area. The area where the landslide occurred is located on a geologic belt (called Chichibu belt) in Shikoku area (Figure 6a) and is characterized by deep river valleys with steep slopes, and many of the mountain slopes have steep chutes. According to the subsurface geological map of Tokushima Prefecture (Tokushima Prefecture, 1983), the area is mainly underlain by Paleozoic greenstone, Paleozoic and Mesozoic pelite and greywacke, and serpentinite of the Mesozoic Kurosegawa terrane, as well as limestone and chert. Figure 6b shows the geological map of the landslide area. Figure 7 presents two geologic cross-sections along line P1-P2-P3 and line C-C′ (as shown in Figure 5). The landslide occurred mainly within colluvium deposits. However, the basal sliding surface occurred mainly within weathered serpentinite. The landslide was 40 m wide, 100 m long, had maximum depth of about 10 m, and estimated volume of 18 000 m^3. According to the distribution of ground surface cracks and drilling results, it was revealed that the landslide consisted of three sub-blocks (B-I, B-II, and B-III as shown in Figure 5), and the blocks had volumes of about 3400, 3600 and 11 000 m^3, respectively.

Extensometers (E-1, E-2, and E-3) were installed to monitor the movements of the three sub-blocks (Figure 5). Figure 8 shows results of displacement and rainfall monitoring for the period during which the landslide was most active. The displacement monitoring commenced on 10 September 2004, but was stopped from 29 September to 21 October to allow preparation of urgent countermeasures. Nevertheless, several meters of displacement were recorded by each extensometer. The displacement data revealed that landslide movement was very sensitive to rainfall, with acceleration occurring during significant rainfall events and deceleration occurring after rainfall ceased (Figure 8). Displacement rates when the landslide was nearly continuously active (10 September–10 December 2004) were 1–5 mm h^{-1} in the absence of rainfall

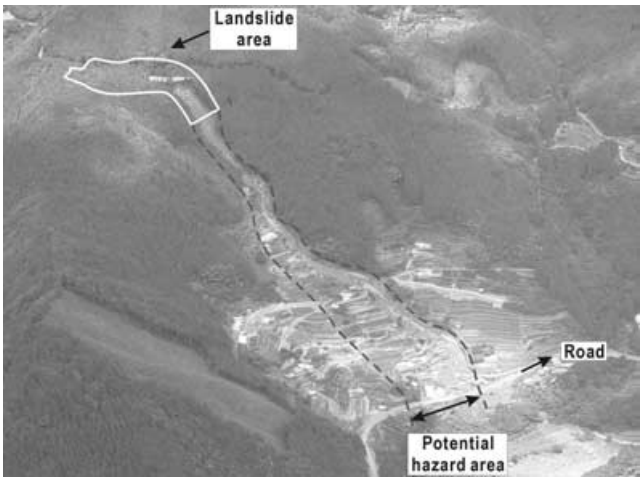

Figure 4. Landslide and potential hazard area in the Furon Valley, August 2004.

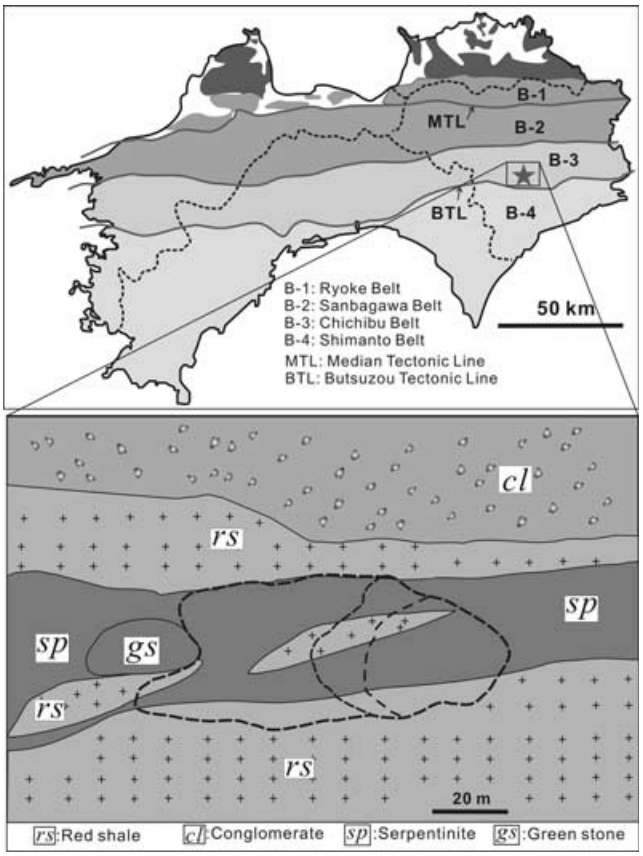

Figure 6. Geological map of the landslide area. (a) Shikoku area, (b) Shiraishi landslide area.

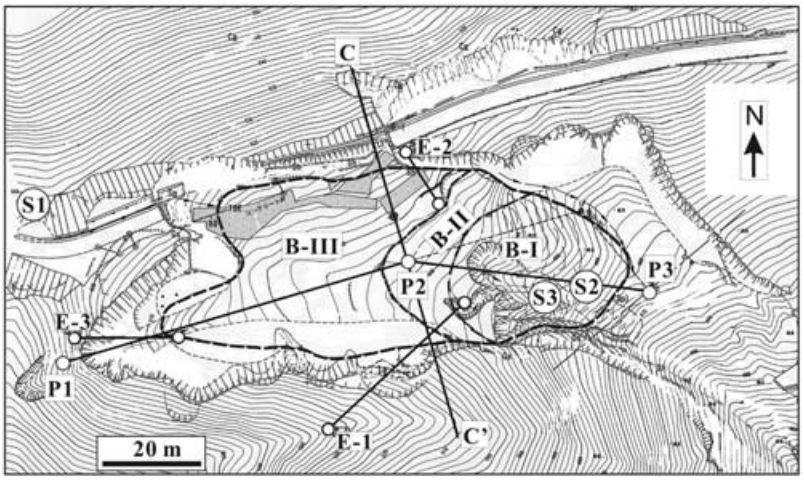

Figure 5. Map of landslide area (marked by heavy dashed lines) and the locations of extensometers (E-1, E-2, and E3) and sampling (S1, S2, and S3)

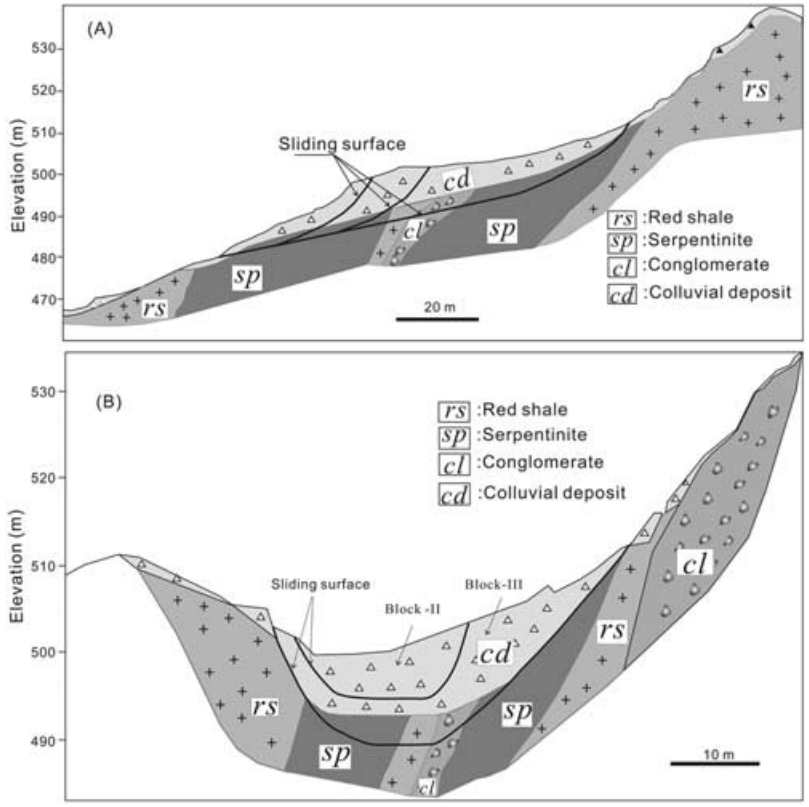

Figure 7. (a) Longitudinal section of landslide along line P1-P2-P3, and (b) cross-section along line C-C′ in Figure 5.

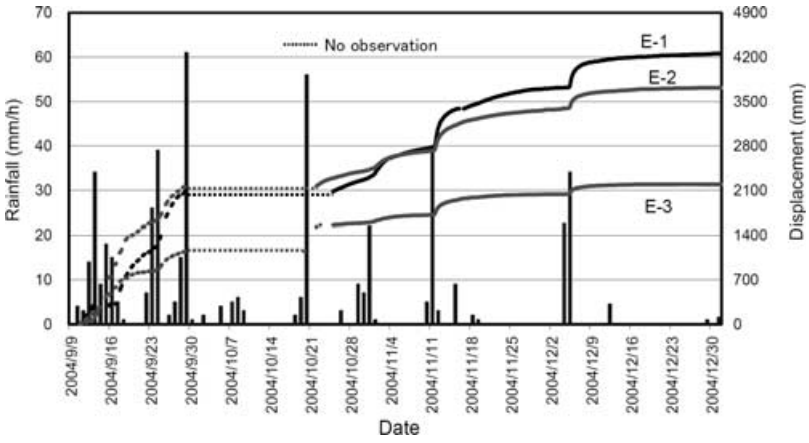

Figure 8. Landslide displacement monitored by extensometers and rainfall during the period 9 September to 31 December 2004.

and 6–28 mm h^{-1} during rainfall. Monitoring of the groundwater table in a borehole at point P2 (shown in Figure 5) revealed that there was a time lag between the responses of landslide displacement and groundwater table during rainfall (Figure 9). The displacement data clearly showed secondary creep (after point T1) and tertiary creep (after point T2). Nevertheless, no rapid, catastrophic failure occurred. Further, the landslide showed a sharp decrease in the displacement rate after point T3, irrespective of the high groundwater table. These movement characteristics differ from the continuous, very slow, creeping movement typical for landslides in serpentinite areas of Japan (Sokobiki *et al.*, 1994; Yatabe *et al.*, 1991, 1997; Yokota *et al.*, 1995, 1997, 1999). The accelerating and decelerating motion suggests possible shear-rate dependent strength properties as reported by others for various clayey soils (Skempton, 1964; Kenney, 1977; Lemos, 1986; Tika, 1989; Tika *et al.*, 1996; Yatabe *et al.*, 1997; Suzuki *et al.*, 2004; Saito *et al.*, 2007).

Laboratory Testing

The unusual movement characteristics of the Shiraishi landslide were evaluated through ring shear testing. The ring shear apparatus has been widely used in measuring the residual shear strength of soils for the analysis of slope stability (Bishop *et al.*, 1971; Bromhead, 1979; Tika and Hutchinson, 1999). Recently, a series of ring shear apparatus was developed and improved by the Disaster Prevention Research Institute (DPRI), Kyoto University (Sassa *et al.*, 2004). These apparatuses enable shearing at different types of loadings under either drained or undrained conditions. Two ring shear apparatuses were used for the present research. One has a shear box with 120 mm inner diameter, 180 mm outer diameter, 115 mm height, and a maximum shear velocity of 10 cm s^{-1}; the other has a shear box with 210 mm inner diameter, 290 mm outer diameter, 95 mm height, and a maximum shear velocity of 18 cm s^{-1}. These apparatuses have a special structure that prevents soil

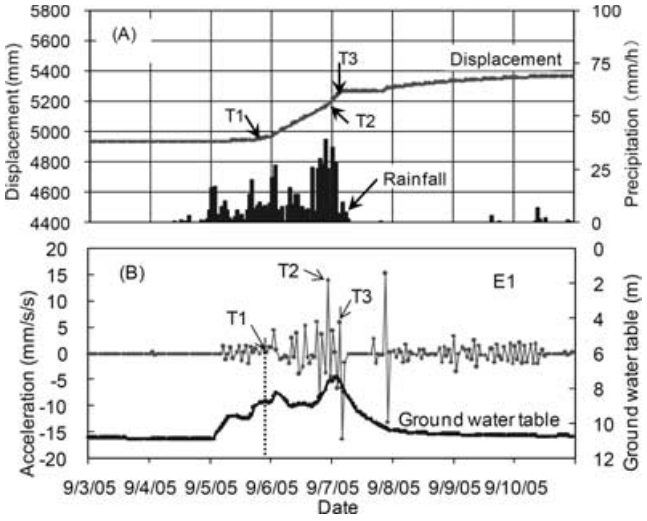

Figure 9. Monitored landslide displacement and ground water table below the ground surface at point P2 (shown in Figure 5) during the period 3–10 September 2005. (a) Rainfall and displacement; (b) groundwater table and acceleration for block BI.

Table I. Properties of the samples

Sample	Density (g cm^{-3})	Liquid limit (%)	Plastic limit (%)	Clay content (%)
S1	2·70	–	–	–
S2	2·70	21	14·7	18
S3	2·73	48	16	33

– Not measured, because the sample does not contain clay.

Table II. Major minerals in the tested samples, determined by X-ray diffraction

Sample	Serpentine	Talc	Chlorite	Smectite
S1	+ + + +	+ +	+ +	+
S2	+ + +	+ +	+ +	+ + +
S3	# # #	#	# # # #	

+, #: Relative content of minerals with greater content indicated by greater number of symbols. Note that S3 was analyzed by Tamura *et al.* (2006); they grouped the interstratified minerals chlorite and smectite.

and water leakage during long displacement, which is a common problem for many other ring shear apparatuses. For additional detail on the design and construction of this ring-shear apparatus, as well as the operating method; refer to Sassa *et al.* (2003, 2004).

We obtained samples for ring shear testing from outside of the landslide (S1), from the landslide body near the basal sliding surface (S2), and directly from the basal sliding surface (S3) (Figure 5). We removed from the samples particles with diameter greater than 4·75 mm due to the size limitation of the shear box. The excluded materials comprised 25·3%, 6·7% and 1·5% by weight of samples S1, S2 and S3, respectively. Yatabe *et al.* (1991) examined the influence of particle size distribution on the residual shear strength of clayey soils and concluded that the residual shear strength was mainly controlled by the matrix material when the sand content was less than 30%. Therefore, we assume that our exclusion of particles with diameter greater than 4·75 mm had negligible effect on the residual shear strengths of the samples. Table I shows index properties of the samples. Table II presents the main clay minerals of the samples determined by X-ray diffraction.

Test specimens for samples S1 and S2 were prepared by pouring oven-dried soil into the shear box in layers and compacting the layers to different densities (Ishihara, 1993). Sample S3 was placed into the shear box as a water-laden slurry. All saturated test specimens were saturated by CO_2 and de-aired water. Sample S1 was tested in both dry and saturated conditions. All specimens were consolidated under a given normal stress and then sheared to residual state using a shear-speed-controlled method. For measurement of residual strength properties, samples S1 and S3 were tested at discrete normal stresses, while sample S2 was tested first at the maximum normal stress and thereafter was sheared at constant rate while the normal stress was decreased very slowly. The residual strength tests were performed at a rate of 0·11 mm min^{-1}. Although the Japanese Geotechnical Society (1987) suggests that residual strength parameters measured using direct shear methods employ a shear rate of 0·02 mm min^{-1}, Yokota *et al.* (1995) found that, for ring shear tests, shear rates below 1·01 mm min^{+1} do not affect the residual shear strength. We performed multistage testing, which has been found to produce results similar to testing of individual samples (Luipini *et al.*, 1981; Bromhead, 1992; Stark and Eid, 1994; Tika *et al.*, 1996; Harris and Watson, 1997; Suzuki *et al.*, 2004; Tiwari and Marui, 2004). Following measurement of residual strength parameters, we performed tests on each sample at various rates to explore possible rate dependence on shear strength. We performed these tests with each sample fully saturated, and also tested sample S1 in a dry state under drained conditions.

Geotechnical index properties (density, Atterberg limits, grain size distributions) were measured for all samples prior to shear testing. Grain size distribution, Atterberg limits, and residual strength tests were also performed on the shear zone developed during ring shear testing of sample S2. A laser microscope and a scanning electron microscope (SEM) were used to observe and measure the shear zone developed in this sample. These observations were made after the sample was sheared at its lowest rate. The SEM was of a new type that enables the direct observation of the shear surface without extra preparation (e.g. evaporation coating) as required by traditional SEM techniques.

Test Results

Residual shear strengths were reached within about 40 mm of displacement (Figure 10). Figures 11–13 show residual strength envelopes for the three samples when tested under saturated conditions. Samples S1, S2 and S3 had residual angles of internal friction (ϕ_r) of 30, 20 and 16°, respectively. Samples S2 and S3 had residual cohesion (c_r) of about 5 kPa and 10 kPa, respectively. Figures 14 and 15 show the variation of residual strengths with shear rate. As indicated by the figures, residual shear strength increased with shear rate. The behavior of sample S1 was similar when both saturated and dry (Figure 14).

A shear zone with slickensided shear surfaces was formed during each test (Figure 16). The soils above the shear zones were removed to permit observation of the upper parts of the shear zones prior to taking the photographs shown in Figure 16. The shear zones were finer grained and differed in color from the unsheared soil above and below. Grain size distribution tests on the shear zone and adjacent material from sample S2 (Figure 16a) demonstrates this finer nature of the shear zones (Figure 17). The liquid limit of the sample S2 shear zone

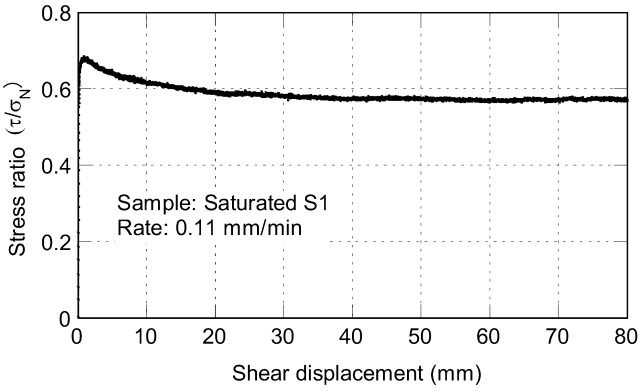

Figure 10. Drained shear test on saturated sample S1.

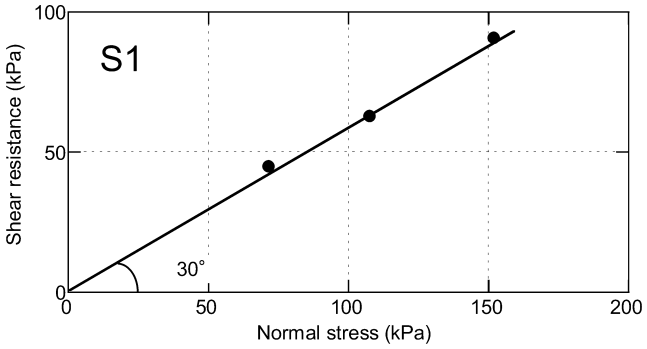

Figure 11. Residual shear strength against normal stress for saturated sample S1.

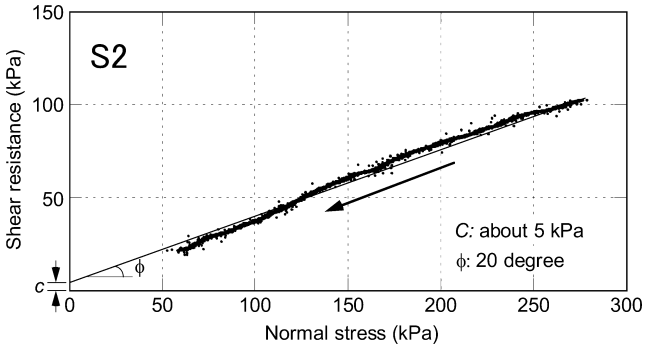

Figure 12. Residual shear strength against normal stress for saturated sample S2.

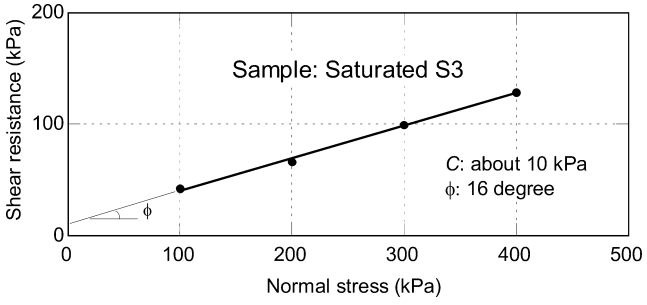

Figure 13. Residual shear strength against normal stress for saturated sample S3.

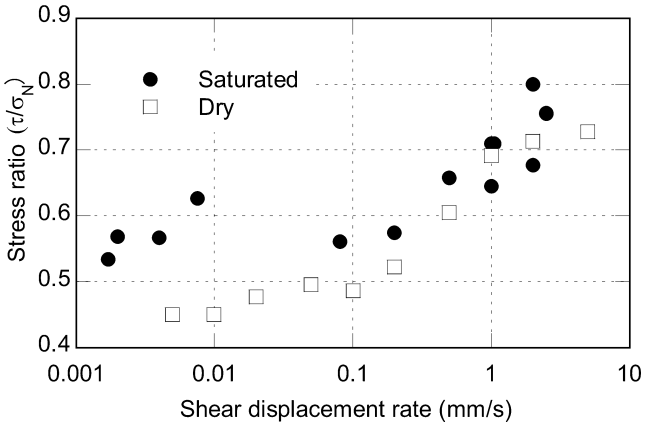

Figure 14. Residual shear strength against shear rate for sample S1 in both saturated and dry states.

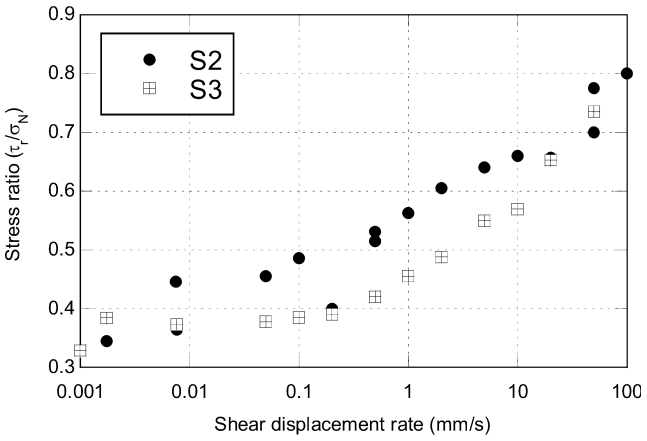

Figure 15. Residual shear strength against shear rate for samples S2and S3.

was 62·0, which is approximately three times greater than that of the original sample. The plastic limit was unchanged by shearing. Ring shear tests performed only on the sample S2 shear zone provided an angle of internal friction of about 13° and 13 kPa of cohesion (Figure 18); these parameters for the original, unsheared sample were 20° and 5 kPa, respectively (Figure 12). Visual observations of the shear zones assisted by the laser and scanning electron microscopes indicated that particles in the shear zones had ordered texture, with platy particles (inferred to be talc and chlorite minerals) aligned parallel to the direction of shear (Figures 19–21).

Discussion

Residual shear strength behavior

It has been reported that weathered serpentine composed of antigorite and chrysotile normally has a ϕ_r ranging from 25 to 30° with $c_r = 0$ (Yokota *et al.*, 1997). However, ϕ_r was less than 25° and c_r was not zero for both S2 and S3 (Figures 11 and 12). This is probably due to the intrusion of other minerals, such as talc, chlorite, and smectite. These clay minerals with low shear strength are normally generated along the margins of serpentine belts by hydrothermal alteration, and may have played key roles in landslide triggering within the serpentine belt (Yatabe *et al.*, 1997). As shown in Figures 6 and 7, the serpentinite is located adjacent to shale, conglomerate, and green stone. The weathering of these rocks may

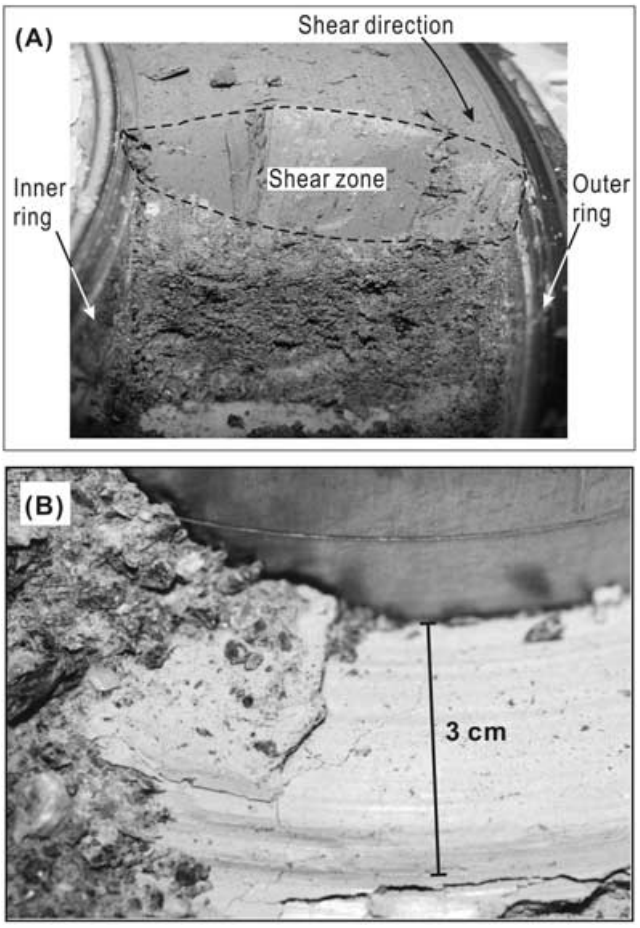

Figure 16. (a) Shear zone from the test on sample S2, and (b) shear zone from the test on dry sample S1.

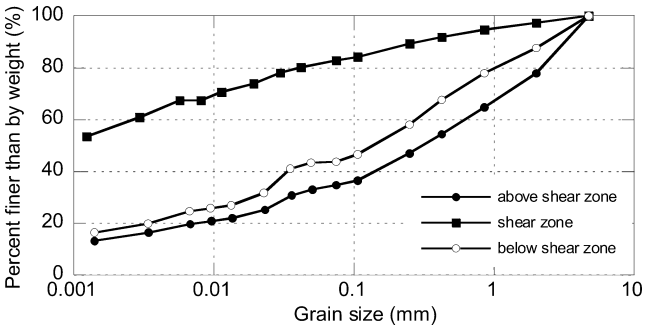

Figure 17. Grain size distribution of the samples that were taken from, above, and below the shear zone shown in Figure 15a.

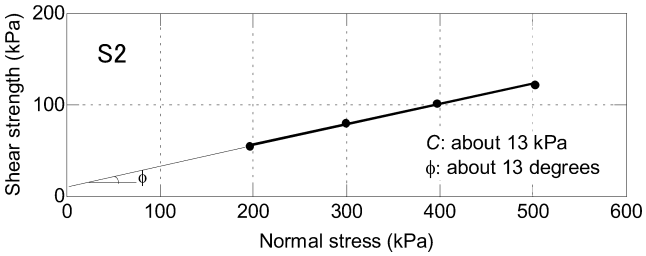

Figure 18. Residual shear strength of the clay from the shear zone shown in Figure 15a.

have introduced talc, chlorite, and smectite into the tested samples, causing the increase in cohesion and decrease in internal friction angle. It is also reported that brucite in serpentinite can be easily eluviated in carbonated water, causing

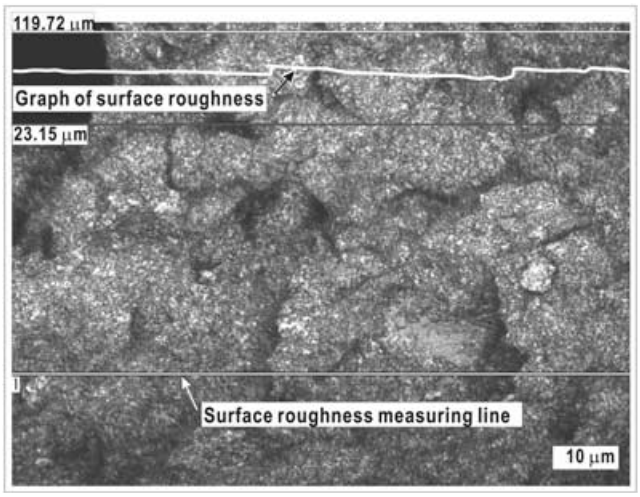

Figure 19. Surface of the shear zone observed by laser microscope.

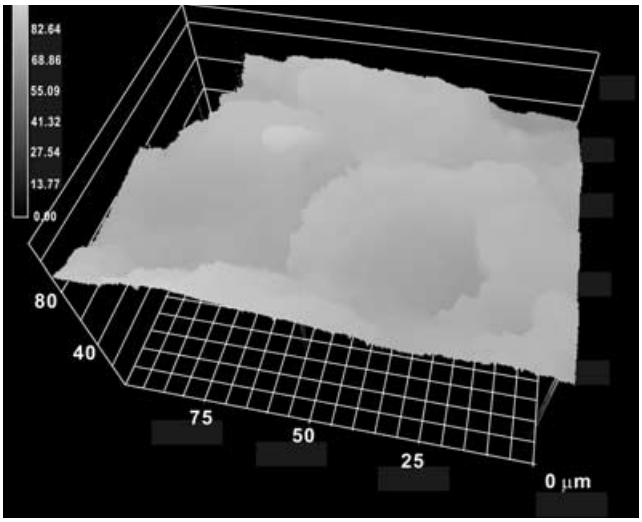

Figure 20. 3D image of the shear zone.

removal of Mg ions and marked decrease of shear resistance (Yokota *et al.*, 1999). Considering that the main parts of the sliding surface for blocks B2 and B3 were probably below the groundwater table for many years, temporal shear strength variation from such eluviation processes should be negligible for the short period of landslide monitoring.

Similar shear tests were performed three times for each sample, and during each test the residual shear strength increased with shear rate as shown for some tests in Figures 14 and 15, although for given specimens there were small variations in the values of ϕ_r and c_r. Detailed discussion of the reasons for these small variations is beyond the scope of this study; however, it is well documented that similar samples may not display identical properties during individual shear tests, even though the samples are collected from the same location (Bromhead, 1992; Harris and Watson, 1997; Tiwari and Marui, 2004).

Traditionally, the shear strength of soil is measured by triaxial testing. However, as discussed previously, soil failure often occurs by localized deformation in a thin zone of intense shearing. Therefore, using the overall stress–strain measurements from triaxial testing would not be representative of such localized, intense shear behavior (Finno *et al.*, 1997). The localized shear zone shown in Figure 16 indicates the advantage of utilizing ring shear tests to mimic the shear behavior

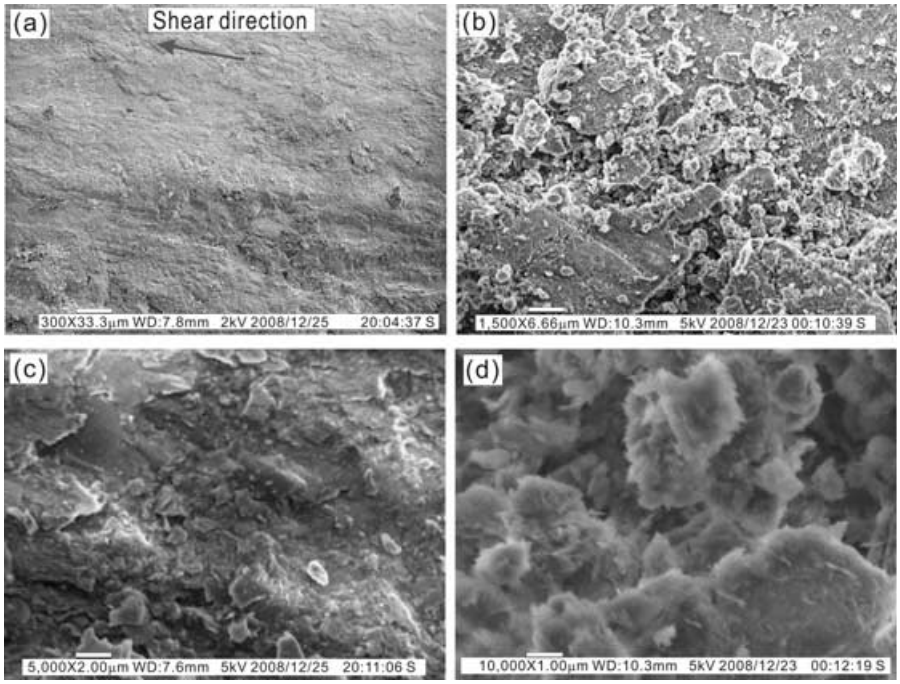

Figure 21. Microstructure of shear zone observed by SEM. (a) ×300, (b) ×1500, (c) ×5000, and (d) ×10000.

of soils along a sliding surface, as detailed by Bishop *et al.* (1971).

The friction angle of soils mobilized during shearing depends on the physical friction and interlocking of soil grains (Lambe and Whitman, 1969). This kind of friction and interlocking also depends on the grain orientation and mode of intergranular shearing (shear mode, Tika *et al.*, 1996). Many studies have been made of the rate effect on residual shear strength of soils (Petley, 1966; Kenney, 1977; Lupini *et al.*, 1981; Osipov *et al.*, 1984; Lemos, 1986; Tika, 1989; Tika *et al.*, 1996; Suzuki *et al.*, 2004; Saito *et al.*, 2007) and three types of variation of the residual strength with increase of shear displacement rate have been recognized: the residual shear strength (a) increases (positive rate effect), (b) decreases (negative rate effect), and (c) does not change (neutral rate effect). Two hypotheses have been proposed to explain the mechanism of shear-rate-dependent residual shear strength of clayey soils, namely (a) excess pore water pressure is produced due to the changing shear rate, which changes effective normal stress and results in changing residual shear strength (The Japanese Geotechnical Society 1987), and (b) the shear mode varies with the shear rate and causes the internal friction angle of soils to change (Skempton, 1985; Tika *et al.*, 1996; Saito *et al.*,2007). According to the variable shear mode hypothesis, the positive rate effect could be explained as follows. During slow shearing, soil grains will become aligned parallel to the shear direction and the shear mode is dominated by intergranular sliding; however, with increasing shear rate, grains within the shear zone will lose their alignment and turbulent shearing will become dominant, resulting in increased shear strength (Skempton, 1985). In the case of the negative rate effect, Tika *et al.* (1996) explained that soil water content in the shear zone will increase with increasing shear rate, leading to the reduction of shear strength. Saito *et al.* (2007) stated that the structure of the shear zone may vary with displacement rate and that shearing may be controlled mainly by the interaction of sand grains at low shear rates, and by the interaction of clay particles at higher shear rates. Clearly, many aspects concerning the mechanism of shear rate-dependent residual shear strength remain unknown. No one mechanism explains the rate effect for all types of clays and all behaviors.

The similar results from ring shear tests performed on dry and saturated specimens of sample S1 indicate that generation of excess pore-water pressure during shearing was not responsible for observed strength changes with shear rate. Therefore, it is reasonable to infer that characteristics of these serpentinite samples that affect shear mode play a key role in the shear-rate-dependent shear strength. Geotechnical properties of the samples changed significantly during initial shearing, as indicated by changed index properties and suggested by changed strength properties. Clay content appears to have been increased during shearing, as indicated by the increased liquid limit and fine content of the shear zone (Figure 20). This increase in clay content was probably due to particle breakage during shearing, as reported by other researchers (Wang and Sassa, 2000; Feda, 2002; Luzzani and Coop, 2002; Okada *et al.*, 2003, Agung *et al.*, 2004; among others), and/or due to larger grains being ejected from the shear zone. The reduction of the internal friction angle and increased cohesion of the sample S2 shear zone compared with the original sample also suggest an increase in clay content.

The alignment of clay particles in the shear zones as observed using the laser and scanning electron microscopes suggests that a change of shear mode, say from sliding shear at low shear rate to turbulent shear at fast shear rate, may be the main reason for the positive rate effect on the residual shear strength.

Rate Dependence of Residual Shear Strength and Observed Landslide Behavior

In the time prediction of landslide occurrence, the method based on the creep rupture theory has been proposed and widely used (Saito and Uezawa, 1966; Fukuzono, 1985; Hayashi *et al.*, 1988; Voight, 1989). Also, the viscous creep behavior of landslides had been studied in detail (van Asch, 1984, 2005; van Asch *et al.*, 1989, 2007; Moeyersons, 1989;

Pieter *et al.*, 1989; Roering, 2004; Ancey, 2007, Sosio *et al.*, 2007). The method based on creep rupture theory uses the displacement rate during the latter stage of secondary creep and the onset of tertiary creep to predict the rupture failure time. For the Shiraishi landslide, although the sliding had characteristics of the latter stage of secondary creep and the early stage of tertiary creep during nearly all heavy rainfall events, there was no catastrophic rupture failure, even though the accumulated displacement reached several meters. In addition to the possible effects of elevated pore-water pressures during rainfall, the shear-rate-dependent residual shear strength may have played a key role in the movement behavior, as follows. During rainfall, the groundwater table rises with the infiltration of rainwater, resulting in the reduction of effective normal stress. This will reduce the shear strength and result in landslide acceleration. However, acceleration will elevate the shear strength of soil along the sliding surface and cause landslide deceleration, such that catastrophic rupture failure cannot occur. This deceleration will then result in the reduction of shear strength and may lead to an additional cycle of landslide acceleration. Therefore, this kind of decelerating and accelerating movement can occur repeatedly. For the Shiraishi landslide, although the landsliding rate calculated from the monitoring data was smaller than the rates used during shear tests, the actual sliding rate might have been greater. Recent displacement monitoring of Slumgullion landslide in the USA revealed that a short-term sliding rate of 100 cm day^{-1} could be reached although the daily displacement was only 1 cm (Schulz *et al.*, 2009); the calculated sliding rate depends on the sampling frequency of the monitoring data. For the Shiraishi landslide, the displacement data were obtained once per hour. Therefore, it is reasonable to believe that the momentary sliding rate may be as great as the rates at which our tests were performed. We acknowledge the problems in using ring shear test results to predict the mobility of slow-moving landslides as pointed out by Van Asch *et al.* (2007). Therefore, displacement monitoring of creeping landslides in serpentinite belts with higher precision and sampling frequency is planned for better understanding of the actual landsliding rate.

Conclusions

A series of ring shear tests was performed on weathered serpentinite samples taken from the Shiraishi landslide area. The basic shear behavior of these samples was examined by shearing them at different normal stresses and shear displacement rates. The results can be summarized as follows.

(1) Samples with different clay minerals showed different shear behavior. Sample S1 from the outside of the landslide showed an internal friction angle of 30°, while sample S2 from the landslide body and S3 near the sliding surface had internal friction angles of 20 and 16°, respectively.
(2) The residual shear strengths for all samples increased significantly with increased shear rate. This includes tests performed on a dry sample, indicating that generation of excess pore-water pressures was not responsible for the observed strengthening with increased shear rate.
(3) In each test, a shear zone formed after long shear displacement. The soil within the shear zone became very clayey and showed lower internal friction angles. Examination of shear-zone microstructure revealed that the change from sliding shear to turbulent shear may be the mechanism of the displacement-rate-dependent shear strength.
(4) The increase of residual shear strength with shear rate may be the key reason for that the observed behavior of the Shiraishi landslide, which experienced accelerating–decelerating movement repeatedly without catastrophic rupture failure, even when the accumulated displacement reached more than several meters within a short period.

Acknowledgements—This study was funded by a scientific research grant (No. 18380094) from the MEXT of Japan. Tokushima Prefecture is thanked for their permission to publish the survey and monitoring results of the landslide. The authors are grateful to the Nanbu General Bureau of Tokushima Prefecture, the previous public office of Kisawa Village, and Mr Tamura in Yonden Consultants Inc., for their help in the field work and sampling. The microstructure of the shear zone was observed using the SEM technique in Mountain Hazard Section of Disaster Prevention Research Institute, Kyoto University. Dr Tairo Yamasaki, JSPS post-doctoral fellow in Disaster Prevention Research Institute, Kyoto University, is thanked for his help in the X-ray diffraction analysis of minerals. Finally, the authors' special thanks go to the associate editor and referees of this paper, for their useful comments used to revise the manuscript.

References

Agung MW, Sassa K, Fukuoka H, Wang G. 2004. Evolution of shear-zone structure in undrained ring-shear tests. *Landslides* **1**(2): 101–112.

Ancey C. 2007. Plasticity and geophysical flows: a review. *Journal of Non-Newtonian Fluid Mechanics* **142**: 4–35.

Bishop AW, Green GE, Garge VK, Andersen A, Brown JD. 1971. A new ring shear apparatus and its application to the measurement of residual strength. *Géotechnique* **21**: 273–328.

Bromhead EN. 1979. A simple ring-shear apparatus. *Ground Engineering* **12**(5): 40–44.

Bromhead EN. 1992. *Stability of Slopes*, 2nd edn. Surrey University Press: London.

Feda J. 2002. Notes on the effects of grain crushing on the granular soil behavior. *Engineering Geology* **63**(1–2): 93–98.

Finno RJ, Harris WW, Mooney MA, Viggiani G. 1997. Shear bands in plane strain compression of loose sand. *Géotechnique* **47** (1): 149–165.

Fukuzono T. 1985. A new method for predicting the failure time a slope. *Proceeds of 4th International.Conference and Field Workshop on Landslides,* Tokyo; 145–150.

Harris AJ, Watson PDJ. 1997. Optimal procedure for the ring shear test. *Ground Engineering* **30**: 26–28.

Hayashi S, Park B, Komamura F, Yamamori T. 1988. On the forecast of time to failure of slope (II) – approximate forecast in the early period of the tertiary creep. *Journal of Japan Landslide Society* **23**(3): 1–16 (in Japanese).

Hiura H, Kaibori M, Suemine A, Satofuka Y, Tsutsumi D. 2004. Sediment-related disasters in Kisawa-Village and Kaminaka-Town in Tokushima Prefecture, Japan, induced by the heavy rainfall of the Typhoon Namtheun in 2004 (prompt report). *Journal of the Japan Society of Erosion Control Engineering* **57**(4): 39–47.

Ishihara K. 1993. Liquefaction and flow failure during earthquakes. *Géotechnique* **43**: 351–415.

Japanese Geotechnical Society. 1987. *Manual of Soil Strength and Geotechnical Failure.*

Kenney TC. 1977. Residual strength of mineral mixtures. *Proceedings of the 9th ICSMFE*; 155–160.

Lambe TW, Whitman RV. 1969. *Soil Mechanics*. John Wiley & Sons, Inc.

Lemos LJL. 1986. The effect of rate on the residual strength of soil. PhD thesis, University of London.

Lupini JF, Skinner AE, Vaughan PR. 1981. The drained residual strength of cohesive soils. *Géotechnique* **31**: 181–213.

Luzzani L, Coop MR. 2002. On the relationship between particle breakage and the critical state of sands. *Soils and Foundations* **42**(2): 71–82.

Moeyersons J. 1989. A possible causal relationship between creep and sliding on Rwaza Hill, southern Rwanda. *Earth Surface Processes and Landforms* **14**: 597–614.

Nakagawa River Office, Shikoku Development Bureau, Ministry of Land, Infrastructure, Transport, and Tourism, Japan. 2004. The flood situation on the downstream of Kanagawa river due to the 2004 Typhoon No. 10 (Namtheum) (in Japanese). at website: (http://www.skr.mlit.go.jp/nakagawa/)

Okada Y, Sassa K, Fukuoka H. 2003. Excess pore pressure and grain crushing of sands by means of undrained and naturally drained ring-shear tests. *Engineering Geology* **75**: 325–343.

Osipov VI, Nikolaeva SK, Sokolov VN. 1984. Microstructural changes associated with thixotropic phenomena in clay soils. *Géotechnique* **34**(2): 293–303.

Petley DJ. 1966. The shear strength of soils at large strains. PhD thesis, University of London.

Pieter MB. Van Genuchten, Helenus De Rijke. 1989. On pore water pressure variations causing slide velocities and accelerations observed in a seasonally active landslide. *Earth Surface Processes and Landforms* **14**: 577–586.

Roering JJ. 2004. Soil creep and convex-upward velocity profiles: theoretical and experimental investigation of disturbance-driven sediment transport on hillslopes. *Earth Surface Processes and Landforms* **29**: 1597–1612.

Saito M, Uezawa H. 1966. Forecasting the time of occurrence of a slope failure. *Journal of Japanese Landslide Society* **2**(2): 7–12 (in Japanese).

Saito R, Sassa K, Fukuoka H. 2007: Effects of shear rate on the internal friction angle of silica sand and bentonite mixture samples. *Journal of Japanese Landslide Society* **44**(1): 33–38 (in Japanese).

Sassa K, Wang G, Fukuoka H. 2003. Performing undrained shear tests on saturated sands in a new intelligent type of ring shear apparatus. *Geotechnology Testing Journal* ASTM **26**: 257–265.

Sassa K, Fukuoka H, Wang G, Ishikawa N. 2004a. Undrained dynamic-loading ring-shear apparatus and its application to landslide dynamics. *Landslides* **1**(1): 1–13.

Schulz WH, McKenna JP, Kibler JD, Biavati G. 2009. Relations between hydrology and velocity of a continuously moving landslide – evidence of pore-pressure feedback regulating landslide motion? *Landslides* **6**(2): 181–190.

Skempton AW. 1964. Long-term stability of slopes. *Géotechnique* **14**: 75–101.

Skempton AW. 1985. Residual strength of clays in landslides, folded strata and the laboratory. *Géotechnique* **35**: 3–18.

Sokobiki H, Yokota K, Yamada T, Tanaka H. 1994. The serpentine landslides in Japan and their characteristics. *Proceedings of the 33rd Japanese Landslide Society Annual Research Presentation Symposium*; 78–81.

Sosio R, Crosta GB, Frattini P. 2007. Field observations, rheological testing and numerical modelling of a debris-flow event. *Earth Surface Processes and Landforms* **32**: 290–306.

Stark TD, Eid HT. 1994. Drained residual strength of cohesive soils. *Journal of Geotechnical Engineering* **123**(5): 335–343.

Suzuki M, Kobayashi K, Yamamoto T, Matsubara T, Hukuda J. 2004. Influence of shear rate on residual strength of clay in ring shear test. *Research Report, School of Engineering, Yamaguchi University* **55**(2): 49–62.

Tamura E, Seto F, Asano S. 2006. Investigation of a serpentine landslides after a debris event and the countermeasures. In *The 2004 Geohazards Occurred in Naka Town of Tokushima Prefecture. Proceedings of the 2006 Field Trip of Japan Landslide Society, Kansai Branch*; 27–67.

Tika TE. 1989. The effect of rate of shear on the residual strength of soil. PhD thesis, University of London.

Tike TE, Hutchinson JN. 1999. Ring shear tests on soil from the Vaiont landslide slip surface. *Géotechnique* **49**(1): 59–74.

Tika TE, Vaughan PR, Lemos L. 1996. Fast shearing of pre-existing shear zone in soil. *Géotechnique* **46**: 197–233.

Tiwari B, Marui H. 2004. Objective oriented multistage ring shear test for shear strength of landslide soil. *Journal of Geotechnical and Geoenvironmental Engineering* **130**: 217–222.

Tokushima Prefecture. 1983. *Subsurface Geological Map*: *Kumosoyama*. Naigai Map Co. Ltd

Van Asch ThWJ, Deimel MS, Haak WLC, Simon J. 1989. The viscous creep component in shallow clayey soil and the influence of tree load on creep rates. *Earth Surface Processes and Landforms* **14**: 557–564.

Van Asch Th WJ. 1984. Creep processes in landslides. *Earth Surface Processes and Landforms* **9**: 573–583.

Van Asch TWJ. 2005. Modelling the hysteresis in the velocity pattern of slow-moving earth flows: the role of excess pore pressure. *Earth Surface Processes and Landforms* **30**: 403–411.

Van Asch ThWJ, Van Beek LPH, Bogaard TA. 2007. Problems in predicting the mobility of slow-moving landslides. *Engineering Geology* **91**: 46–55.

Voight B. 1989. A relation to describe rate-dependent material failure. *Science* **243**(4888): 200–203.

Wang FW, Sassa K. 2000. Relationship between grain crushing and excess pore pressure generation by sandy soils in ring shear tests. *Journal of Natural Disaster Science* **22**(2): 87–96.

Wang G, Suemine A, Furuya G, Kaibori M, Sassa K. 2005. Rainstorm-induced landslides in Kisawa Village, Tokushima Prefecture, Japan. *Landslides* **2**: 232–242.

Yatabe E, Yagi N, Enoki M. 1991. The ring shear characteristics of clays from landslides in fractured zone. *Journal of Geotechnical Engineering, Japan Society of Civil Engineering* **436**(III-16): 93–101 (in Japanese).

Yatabe R, Yokoda K, Yagi M, Nochi M. 1997. Consideration on the mechanism of landslides at Serpentine Belt. *Journal of Japanese Landslide Society* **34**(1): 24–30.

Yokoda K, Yatabe R, Yagi N. 1995. Strength characteristics of weathered serpentinite. *Journal of the Japanese Society of Civil Engineers* **529**(III-33): 155–163.

Yokota K, Yatabe R, Yagi N. 1997. Effects of clay minerals and shear strength on the development of serpentine landslides. *Journal of the Japanese Society of Civil Engineers* **568**(III-39): 125–132.

Yokota K, Yatabe R, Yagi N, Yube M. 1999. Consideration from weathering characteristics of serpentine on landslide in serpentine belt. *Journal of Japanese Landslide Society* **36**(2):32–38.